The Journal of Experimental Biology 202, 1741–1752 (1999)
Printed in Great Britain © The Company of Biologists Limited 1999
JEB1914

MECHANICAL *VERSUS* PHYSIOLOGICAL DETERMINANTS OF SWIMMING SPEEDS IN DIVING BRÜNNICH'S GUILLEMOTS

JAMES R. LOVVORN[1,*], DONALD A. CROLL[2] AND GEOFFREY A. LIGGINS[3]

[1]*Department of Zoology, University of Wyoming, Laramie, WY 82071, USA*, [2]*Institute of Marine Sciences, University of California, Santa Cruz, CA 95064, USA* and [3]*Department of Mechanical Engineering, University of British Columbia, Vancouver, British Columbia, Canada V6T 1Z4*

*e-mail: lovvorn@uwyo.edu

Accepted 15 March; published on WWW 8 June 1999

Summary

For fast flapping flight of birds in air, the maximum power and efficiency of the muscles occur over a limited range of contraction speeds and loads. Thus, contraction frequency and work per stroke tend to stay constant for a given species. In birds such as auks (Alcidae) that fly both in air and under water, wingbeat frequencies in water are far lower than in air, and it is unclear to what extent contraction frequency and work per stroke are conserved. During descent, compression of air spaces dramatically lowers buoyant resistance, so that maintaining a constant contraction frequency and work per stroke should result in an increased swimming speed. However, increasing speed causes exponential increases in drag, thereby reducing mechanical *versus* muscle efficiency.

To investigate these competing factors, we have developed a biomechanical model of diving by guillemots (*Uria* spp.). The model predicted swimming speeds if stroke rate and work per stroke stay constant despite changing buoyancy. We compared predicted speeds with those of a free-ranging Brünnich's guillemot (*U. lomvia*) fitted with a time/depth recorder. For descent, the model predicted that speed should gradually increase to an asymptote of 1.5–1.6 m s^{-1} at approximately 40 m depth. In contrast, the instrumented guillemot typically reached 1.5 m s^{-1} within 10 m of the water surface and maintained that speed throughout descent to 80 m. During ascent, the model predicted that guillemots should stroke steadily at 1.8 m s^{-1} below their depth of neutral buoyancy (62 m), should alternate stroking and gliding at low buoyancies from 62 to 15 m, and should ascend passively by buoyancy alone above 15 m depth. However, the instrumented guillemot typically ascended at 1.25 m s^{-1} when negatively buoyant, at approximately 1.5 m s^{-1} from 62 m to 25 m, and supplemented buoyancy with stroking above 25 m. Throughout direct descent, and during ascent at negative and low positive buoyancies (82–25 m), the guillemot maintained its speed within a narrow range that minimized the drag coefficient.

In films, guillemots descending against high buoyancy at shallow depths increased their stroke frequency over that of horizontal swimming, which had a substantial glide phase. Model simulations also indicated that stroke duration, relative thrust on the downstroke *versus* the upstroke, and the duration of gliding can be varied to regulate swimming speed with little change in contraction speed or work per stroke. These results, and the potential use of heat from inefficient muscles for thermoregulation, suggest that diving guillemots can optimize their mechanical efficiency (drag) with little change in net physiological efficiency.

Key words: guillemot, *Uria* spp., swimming speed, muscle efficiency, drag, buoyancy, quasi-steady model, diving, biomechanics, locomotion, stroke–glide cycle, gliding.

Introduction

For bird flight in air, it is often assumed that normal cruising speed corresponds to the speed of minimum cost of transport (COT, J kg^{-1} m^{-1}, Pennycuick, 1987a; but see Pennycuick, 1997). For underwater flight, speeds of minimum COT were also preferred by penguins swimming horizontally without changes in buoyancy with depth (Culik and Wilson, 1991). However, during vertical dives when buoyant resistance changes dramatically with compression of air spaces, it is unclear how mechanical and physiological variables are regulated to minimize transport costs. In birds such as auks (Alcidae) that fly both in air and under water, the physiological efficiency of muscle contraction and the mechanical efficiency of thrust production may not be maximized at the same stroke frequencies and speeds. In the present study, we investigate how auks modulate vertical swimming speeds to mediate physiological and mechanical efficiencies as buoyancy changes.

Muscle fiber types have not been studied in auks, but in other birds with sustained, fast, flapping flight, the flight muscles are

composed almost entirely of fast fibers (Goldspink, 1981; Turner and Butler, 1988; Torella et al., 1996). All these fibers have their highest power output and efficiency [work/(work+heat)] in a relatively narrow range of contraction speeds and loads (Hill, 1950, 1964; Rome et al., 1988; Pennycuick, 1992). If stroke cycles are divided equally between extension and contraction, with no variable glide phase, then changes in contraction frequency imply changes in contraction speed (Pennycuick, 1991); thus, wingbeat frequency must also stay within a narrow range to avoid large declines in power output and efficiency (Goldspink, 1977, 1981; Pennycuick, 1990, 1992, 1996). However, when birds flying in air lose weight so that less power is needed, they often avoid changing their contraction speed and work per stroke by alternately flapping and gliding (Pennycuick, 1991). Penguins swimming under water also glide between strokes (Clark and Bemis, 1979), so that changes in stroke frequency do not necessarily imply changes in contraction speed or work per stroke.

In guillemots (*Uria* spp., Alcidae), wingbeat frequencies in air (≈8.7 Hz) are much higher than under water (1.9–2.8 Hz), so their muscles cannot be well adapted to stroke frequencies in both media (Pennycuick, 1987b). Salt water is over 800 times denser than air at sea level, and the greater resistance demands a lower contraction speed (Pennycuick, 1991, 1992). Assuming that their muscles are adapted mainly to aerial flight, and considering that efficiency drops dramatically below the optimum contraction speed, the flight muscles of guillemots may be quite inefficient under water regardless of variations in contraction speed or frequency. Moreover, part of the 'waste' heat of inefficiency from exercising muscles can substitute for the costs of thermoregulation (for a review, see Bruinzeel and Piersma, 1998). Thus, the efficiency of muscle contraction and thermoregulation combined may be high despite a low efficiency of the locomotor muscles (Hind and Gurney, 1997).

As diving birds descend, the increasing compression of respiratory and plumage air spaces greatly lowers buoyant resistance (Lovvorn and Jones, 1991a; Wilson et al., 1992). Thus, if constant stroke frequency and work per stroke are maintained, swimming speed should increase with increasing depth. However, hydrodynamic drag increases exponentially with increasing speed, causing a rapid loss of mechanical efficiency. Thus, it might be better to minimize the waste heat of drag that cannot be recovered, rather than heat from inefficient muscles that is usable for thermoregulation (Chai et al., 1998). Optimizing drag rather than stroke frequency would be favored if changes in stroke frequency did not require changes in contraction speed or work per stroke, but only altered the duration of gliding.

To investigate the influence of stroke frequency *versus* drag on swimming speed, we developed a biomechanical model of diving for guillemots (*Uria* spp.). This model assumed that stroke frequency and work per stroke stay constant as buoyancy changes with depth. In developing this model, we measured the hydrodynamic drag of a frozen guillemot and wingbeat frequencies from films of Brünnich's guillemots (*U. lomvia*, thick-billed murres) near the beginning of descent. We tested the model predictions against the descent and ascent speeds of a free-ranging Brünnich's guillemot fitted with a time/depth recorder.

Materials and methods

Drag of the body fuselage

The hydrodynamic drag of a frozen common guillemot (*Uria aalge*) was measured in a tow tank. The wings of the guillemot were removed to leave a 'fuselage' of the head and body trunk without propulsive limbs. The feet, which are not used in underwater propulsion by guillemots, were left attached. The bird was mounted on a sharpened steel rod (1 cm diameter) passing through the length of the body and refrozen in a symmetrical diving posture. The guillemot with wings removed had a length from bill tip to tail tip of 0.478 m, a frontal area of 9.860×10^{-3} m^2 and a wetted surface area of 0.0964 m^2 (for measurement methods, see Lovvorn et al., 1991).

The force block was housed in an aluminum cylinder 28 cm long with an outside diameter of 14 cm. An aluminum half-sphere was screwed onto the front of the cylinder, and an aluminum cone 17 cm long was screwed onto the rear of the cylinder. The sting (the rod extending from the rear of the bird) passed through a hole in the half-sphere and was attached to the force block inside the housing. A vertical strut made of aluminum airfoil extrusion (8 cm deep × 3 cm wide) was welded onto the horizontal force-block housing, 17.5 cm from the front of the cylinder. The mounted bird and housing were 50 cm below the water surface, with 15 cm of the sting exposed between the bird and the housing. The strut was bolted to a carriage that towed the assembly in a tank at speeds up to 5 m s^{-1} (for details, see Lovvorn et al., 1991).

The drag of a frozen guillemot with wings removed does not account for the drag of the propulsive wings. In our modeling approach (see Lovvorn et al., 1991), the drag of oscillating propulsors is subsumed by the aerobic efficiency coefficient (η, mechanical power output ÷ aerobic power input). This coefficient is used to calculate the aerobic energy requirements from estimates of the mechanical power needed to propel the body fuselage at quasi-steady speeds (see below). This approach is analogous to that often used in naval engineering, whereby the drag of a hull is matched with a propulsive system of given net efficiency. In our case, this method obviates the need to measure the instantaneous drag of oscillating, rotating limbs throughout a quasi-steady stroke cycle, a task no one has yet accomplished. Note that η subsumes any energy savings through elastic recoil of tendons or other tissues.

We calculated Reynolds numbers (*Re*) for the frozen guillemot of body length L_b (m) at each speed U (m s^{-1}) from $Re=UL_b/\nu$, where ν is the kinematic viscosity of fresh water at 14.5 °C (1.154×10^{-6} m^2 s^{-1}). Drag coefficients (C_D) were calculated as $C_D=2D/\rho A_{sw}U^2$, where D is drag (in N), ρ is the density of fresh water at 14.5 °C (999 kg m^{-3}) and A_{sw} is the wetted surface area (m^2) of the bird.

Buoyancy

The buoyancy of body tissues (0.686 N l^{-1} for lipid, –0.637 N l^{-1} for fresh muscle; see below) is much less than that of air (9.79 N l^{-1}) and, unlike air, the buoyancy of tissues remains essentially constant with water depth. Thus, buoyancy and its variations with depth depend mainly on the volume of air in the respiratory system and plumage (Lovvorn and Jones, 1991a). The fraction by which air volumes are reduced by hydrostatic pressure decreases rapidly with depth: as pressure increases at a constant rate of 10 kPa m^{-1} of depth, air volume decreases by a factor of 10/(n+10) where n is depth in meters. These air volumes are probably manipulated somewhat by the birds depending on its dive depth and fat content (Lovvorn and Jones, 1991a). However, air volumes are difficult to measure in freely diving birds in the laboratory (Stephenson, 1995), and no methods have been devised for measuring them in the field.

The buoyancies of guillemot body tissues were calculated from body composition. Measured by water displacement in a graduated cylinder, the specific volume of fresh pectoral muscles in 20 wild canvasback ducks (*Aythya valisineria*) was 0.939±0.017 l kg^{-1} (mean ± S.D.) (Lovvorn and Jones, 1991a). This value yields a density of 1.065 kg l^{-1} and a buoyancy of –0.637 N l^{-1} or –0.598 N kg^{-1} of fresh muscle. If fresh pectoral muscle contains 26 % protein by mass (Raveling, 1979), then the density of dry protein is (0.26×1.065)/[1–(0.74×1.065)]=1.307 kg l^{-1}. The resulting buoyancy of dry protein is (1 kg l^{-1} of displaced water – 1.307 kg l^{-1} of protein) (9.806 m s^{-2})/(1.307 kg l^{-1})=–2.302 N kg^{-1} or –3.008 N l^{-1}. The density of triglyceride is approximately 0.93 kg l^{-1} (DeVries and Eastman, 1978), corresponding to a specific volume of 1.075 l kg^{-1} and a buoyancy of 0.686 N l^{-1} or 0.738 N kg^{-1} of lipid. We measured the specific volume of ash from a female canvasback duck (including feathers) weighing 0.760 kg and containing 0.040 kg of ash (5.3 %) to be 0.336 l kg^{-1} of ash, giving a density of 2.974 kg l^{-1}. This density yields a buoyancy of –19.353 N l^{-1} of ash or –6.508 N kg^{-1} of ash.

For 25 common guillemots collected in northwest Scotland in November with a mean body mass of 1.0 kg, the fresh body including feathers contained 64.4 % water, 21.7 % protein, 10.2 % lipid and 3.6 % ash (Furness et al., 1994). Ash content was not measured, but lean dry mass was. We assumed the ash content to be 14.2 % of lean dry mass including feathers, on the basis of data for defeathered long-tailed ducks (oldsquaws, *Clangula hyemalis*; Leafloor et al., 1996). Whole-body ash mass is essentially unaffected by whether the feathers are removed before carcass analysis (J. R. Lovvorn, unpublished data). We applied these component percentages to the body mass of 1.087±0.069 kg (mean ± S.D.) for five common guillemots shot near the Semidi Islands, Alaska, USA, in June 1995. With buoyancies of –2.302 N kg^{-1} for dry protein, 0.7381 N kg^{-1} for lipid and –6.508 N kg^{-1} for ash, these percentages yield a buoyancy for body tissues of –0.7158 N for a guillemot weighing 1.087 kg.

For plumage air volume, Wilson et al. (1992) measured the water displacement of dead common guillemots with unflooded plumage and respiratory system, then with flooded plumage, and then with the plumage flooded and all the respiratory spaces punctured and flooded. From these data, they estimated the plumage air volume for guillemots weighing approximately 0.87 kg to be 0.33 l kg^{-1}. This value is only 6 % lower than the value of 0.351 l kg^{-1} estimated for a 1.087 kg bird using the equation for dead redheads (*Aythya americana*) and greater scaup (*A. marila*) in Fig. 4 of Lovvorn and Jones (1991a): plumage air volume (in l)=0.2478+0.1232M_b, where M_b is body mass.

Lacking direct measurements for alcids, Wilson et al. (1992) estimated respiratory volume (V_{resp}, l) from body mass (M_b, kg) using Lasiewski and Calder's (1971) general allometric equation based on non-diving birds, where $V_{resp}=0.1608M_b^{0.91}$ (note that equation 17 in Wilson et al., 1992, gives volume in m^3, not $m^3 kg^{-1}$). By this equation, V_{resp} for a guillemot weighing 1.087 kg is 0.173 l or 0.160 l kg^{-1}. This allometric equation gives the same value (0.165 l kg^{-1}) as that obtained from gas dilution measurements of respiratory volume after expiration in seven live, dive-trained tufted ducks (*Aythya fuligula*) with mean mass of 0.740 kg (Stephenson et al., 1989b). This close agreement suggests that the equation of Lasiewski and Calder (1971) yields good estimates of respiratory volumes after exhalation in 'trained' birds that dive regularly for appreciable distances. Various birds have been reported to exhale immediately before diving (Lovvorn, 1991), so end-expiratory volume appears to be an appropriate measure for our purposes. 'Untrained' tufted ducks that dive irregularly or only for short distances have greater respiratory volumes (0.180–0.232 l kg^{-1}) and lower volumes of blood in which oxygen can be stored in a non-buoyant form (Keijer and Butler, 1982; Stephenson et al., 1989b; Lovvorn and Jones, 1994).

Using the estimated plumage volume of dead diving ducks weighing 1.087 kg (0.351 l kg^{-1}), the respiratory volume for untrained diving ducks (0.180 l kg^{-1}) and the tissue volumes given above yields a total body volume of 1.590 l for a 1.087 kg bird. This value is only 0.9 % lower than that (1.604 l) estimated using the equation in Fig. 1 of Lovvorn and Jones (1991b) for the volume of live, restrained, untrained diving ducks measured by water displacement: total body volume (in l)=0.06574+1.144M_b+0.2495M_b^2. The calculated buoyancy for a 1.087 kg bird of 4.93 N is only 0.6 % lower than that (4.96 N) predicted by the equation in Fig. 1 of Lovvorn and Jones (1991b) based on measured buoyancies of these live, untrained diving ducks: total body buoyancy (in N)=1.21+3.17M_b^2.

Thus, estimates of body volume and buoyancy, based on body composition and predictive equations for air volumes, are very similar (within 1 %) to direct measurements on live, untrained diving ducks. Because dive training causes captive birds to reduce their respiratory volumes after expiration (Stephenson et al., 1989b), and birds commonly sleek their feathers (reducing plumage air volume) before voluntary dives, we used the lower allometric value of 0.160 l kg^{-1} for respiratory volume and 0.33 l kg^{-1} for plumage air volume. These values result in a total body volume of 1.546 l and a net

buoyancy of 4.50 N for a 1.087 kg guillemot at the water surface.

Birds lose some air from the respiratory system and/or plumage during dives, but the amount lost is very difficult to measure. In an impressive set of experiments, Stephenson (1994, 1995) used helium dilution and pressure changes in surface chambers to estimate air volumes lost from the plumage during dives 1.5 m deep by lesser scaup (*Aythya affinis*). However, the response time of the apparatus was too long to detect rapid predive exhalation and ptilosuppression, which are mechanisms commonly used by birds to reduce buoyancy during dives (Lovvorn, 1991). Thus, Stephenson's (1994, 1995) longer-term predive measurements may have overestimated the volumes of air taken down by the birds. Stephenson (1994) also pointed out that the rate of underwater air loss he measured could not continue indefinitely. According to this measured rate, ducks should lose all the air in their plumage within 34 s of submergence, but ducks dive for longer than that without becoming wetted. Because the time course and limits to air loss in deep-diving birds remain unclear, our model does not account for the loss of air from the respiratory system or plumage.

Stroke acceleration curves, inertial work and summation of work components

Using kinematic analyses of high-speed films (100 Hz), Lovvorn et al. (1991) developed a quasi-steady model of stroking by foot-propelled diving ducks. This model integrated the work done by the muscles against drag, buoyancy and inertia throughout the power phase of each stroke. For the present study, no high-speed films of wing-propelled alcids under water were available. As a starting point for modeling, we assumed that the stroke acceleration curves of guillemots resembled those of wing-propelled penguins.

Changes in body fuselage speed (U_b) throughout a single stroke for Humboldt penguins (*Spheniscus humboldti*) were calculated from the thrust of the body (T_c) plotted in Fig. 10 of Hui (1988), and Hui's equation 14: $U_b=(T_c/2.59)^{1/2}$. Hui (1988) found greater thrust during the upstroke than the downstroke in penguins swimming horizontally near the water surface, where high buoyancy must be countered by the upstroke. We reversed this pattern for vertically diving guillemots, which have wings, a skeleton and musculature adapted to downstroke-based aerial flight (Stettenheim, 1959; Raikow et al., 1988; Rayner, 1995). The resulting curve (Fig. 1) corresponded well with patterns crudely inferred from the angles of attack of the wings of common guillemots filmed at 32 frames s^{-1} by Stettenheim (1959, p. 221).

Work during a swimming stroke was modeled by calculating the linear distance moved by the body fuselage during 0.01 s intervals according to the fractional speeds in Fig. 1 and mean swimming speed at a given depth (see below). Work during these 0.01 s intervals was calculated by multiplying the drag and buoyancy at a given depth by the displacement, and then adding the inertial work done in accelerating the body and the added mass of entrained water (see Lovvorn et al., 1991). In quasi-steady fashion, the work during all intervals was then integrated over the entire stroke to yield the total work during the stroke.

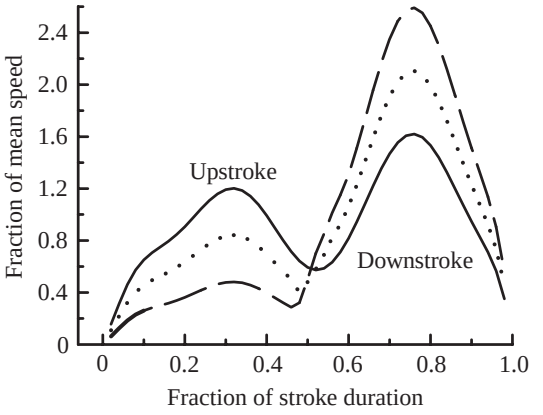

Fig. 1. Fraction of mean swimming speed (F_U) *versus* fraction of stroke duration (F_t) based on thrust curves for Humboldt penguins during horizontal swimming at 1 m s^{-1} (Hui, 1988) (solid line). When applied to auks, the first peak is for the upstroke and the second peak is for the downstroke. The equation is: $F_U=-0.007314+12.552F_t-104.60F_t^2+481.50F_t^3-578.20F_t^4-1807.8F_t^5+4411.2F_t^6-4923.2F_t^8+3581.9F_t^{10}-1075.4F_t^{12}$. Other lines show the curve when the fraction of mean speed during the upstroke was decreased, and the fraction during the downstroke increased, by 30 % (dots) and 60 % (dashes).

Because we had no direct data on acceleration patterns during strokes in guillemots, we evaluated the effects on model estimates of varying the stroke acceleration curve. We varied the shape of the curve twice by altering the regression coefficients by −30 % during the upstroke and +30 % during the downstroke, and then by −60 % during the upstroke and +60 % during the downstroke (Fig. 1). The resulting curves simulated increasing fractions of total thrust being generated during the downstroke *versus* the upstroke.

Stroke rates and stroke distances with changing depth and buoyancy

The speed of common guillemots swimming horizontally in tanks 1 m deep was measured as 2.18±0.43 m s^{-1} (mean ± S.D., N=179 sequences) (Swennen and Duiven, 1991). However, time/depth recorders fitted on vertically diving, free-ranging Brünnich's guillemots (*Uria lomvia* L.) revealed mean speeds of 0.94±0.48 m s^{-1} (N=5534 dives) during descent and 0.86±0.47 m s^{-1} (N=6029 dives) during ascent for a mean dive depth of 18 m (Croll et al., 1992). At shallow depths where buoyancy is high, vertical descent speeds are expected to be slower than horizontal speeds; at deeper depths of low positive buoyancy, passive ascent *via* buoyancy alone will be slower than powered ascent. Croll and McLaren (1993) reported mean wingbeat frequency under water as 1.8–1.9 Hz for guillemots swimming horizontally or at very shallow angles in tanks and in the field.

We measured the wingbeat frequencies of Brünnich's

guillemots descending almost vertically within 4 m of the water surface, using underwater films from Lancaster Sound (National Geographic Society, 1995), located approximately 1225 km north of our Coats Island study area (see below). For each bird, we made 8–10 repeat measurements with a stopwatch of the time required to complete the same sequence of 8–10 strokes, calculated the mean of repeat measurements for that single sequence per bird, and then calculated the overall mean stroke rate among sequences for 20 individual guillemots. The resulting overall value was 2.80±0.03 Hz (mean ± S.E.M., N=20). On the basis of a mean descent speed of 0.94 m s^{-1} (Croll et al., 1992), this value yields an initial stroke distance near the water surface of 0.336 m $stroke^{-1}$.

As a testable hypothesis, our model assumed that stroke frequency (thus stroke duration), work per stroke and stroke acceleration pattern (Fig. 1) remained constant despite changes in buoyancy with depth. Gliding was not included in stroke duration, but rather as time steps after strokes during which no strokes occurred. For each stroke, our model determined how far the body fuselage progressed depending on the net force of constant work per stroke, minus the forces of drag, buoyancy and inertia at the current speed. Decreasing buoyant resistance during the descent resulted in increasing distance per stroke, until greater drag at higher speeds offset the reduced buoyancy. At some depth, compression of the air spaces caused buoyancy to switch from a positive value to a negative value. Buoyancy opposed descent above that depth and augmented descent below that depth; the reverse was true during ascent.

To ascend in shallow water, ducks simply stop stroking, and their buoyancy takes them quickly to the surface (Lovvorn, 1994). In that case, the cost of ascent is only the resting metabolic rate (RMR) during the time required to float upwards. But for guillemots diving to depths of up to 210 m, buoyancy is often only slightly positive or even negative when they begin ascent. At depths of small positive buoyancy, it takes a long time for the small buoyant force to accelerate the birds to an adequate ascent speed. Given that their RMR is quite high in cold water at depth (Kooyman et al., 1976; Grémillet et al., 1998), the cost of waiting for buoyancy to provide sufficient upthrust is greater than the cost of swimming upwards over the same distance in a shorter time. By this argument, active swimming is energetically cheaper until the birds ascend to a depth where the buoyant force is great enough to provide adequate upward speed.

In the model, we assumed that guillemots stop upward swimming and begin passive ascent at the depth that minimizes total cost. At a time step of one stroke duration, the model decided whether it was more cost-effective to ascend actively or passively. At low positive buoyancies, this algorithm resulted in a stroke being followed by varying numers of time steps of passive ascent (gliding). We performed simulations for two stroke durations: 0.357 s measured from films of vertical descent within 4 m of the water surface (see above), and 0.526 s measured for guillemots swimming horizontally or at very shallow angles in tanks and in the field (Croll and McLaren, 1993).

Aerobic costs

To compare energy costs of active *versus* passive ascent, the mechanical costs of active swimming must be converted to aerobic costs. The conversion factor is termed the aerobic efficiency (η) or the mechanical power output/aerobic power input. This factor is determined by measuring rates of oxygen consumption ($\dot{V}_{O_2}$) and modeling mechanical power output under the same conditions. The value of η depends strongly on the mechanical model used, i.e. the same $\dot{V}_{O_2}$ can yield different values of η for different modeling approaches. This dependency results in widely varying η values reported in the literature (Stephenson et al., 1989a). These differences do not necessarily mean that true values of η differ among species or swimming modes, but perhaps only that the mechanical models were not comparable. We used η=0.234, calculated from $\dot{V}_{O_2}$ of tufted ducks diving in water 0.6 m deep at 7 °C (Bevan and Butler, 1992) and a quasi-steady model for ducks similar to the one used here for alcids (Lovvorn et al., 1991).

During passive ascent due to buoyancy, the energy cost was assumed to be the resting metabolic rate (RMR) of guillemots floating on water at 7 °C. Croll and McLaren (1993) described post-absorptive RMRs (in W kg^{-1}) in Brünnich's guillemots floating on water at temperatures (T_w) from 1 to 20 °C using the equation RMR_w=20.99–0.77T_w (r^2=0.82). The absorptive RMR_w in fed Brünnich's guillemots floating on water at approximately 20 °C (13.0 W kg^{-1}) was 43 % higher than post-absorptive values (9.1 W kg^{-1}) (Croll and McLaren, 1993). It is believed that most digestion by guillemots occurs after foraging bouts (see Hawkins et al., 1997), so we did not consider the heat increment of feeding during dives and used only post-absorptive RMR_w. From the above equation for post-absorptive Brünnich's guillemots, the RMR_w at 7 °C ($RMR_{w,7}$) was approximately 2.5 times the RMR in air (Croll and McLaren, 1993). For the body mass of 1.087 kg we used in our model, predicted $RMR_{w,7}$ is 13.56 W kg^{-1}. Lacking measurements, we did not consider the effects of compression of the plumage air layer with depth on RMR_w or aerobic efficiency (see Kooyman et al., 1976; Grémillet et al., 1998).

Vertical speeds of free-ranging guillemots

Electronic time/depth recorders were deployed on eight adult Brünnich's guillemots nesting on cliffs at Coats Island in northern Hudson Bay, Canada, in July–August 1988–1989 (for details, see Croll et al., 1992). Recorders were 6 cm long × 2.5 cm wide × 1.5 cm high, weighed 35 g, and were tapered at the ends. Recorders were attached along the middle of the back, with 5 min epoxy adhesive, and were worked well into the feathers to reduce profile drag. Every 4 s, a transducer measured pressure, which was converted to depth with a resolution of 1.3 m. Depths shallower than 3 m were not recorded. Descent and ascent rates were calculated from depth changes over each 4 s interval. After the birds had returned from foraging trips, the recorders were retrieved. We chose one complete period away from the nest by a representative bird for analysis of dive patterns.

The foraging period by the individual guillemot we examined included 123 dives to over 3 m depth. We defined the period of 'direct descent' as that during which depth increased monotically with ⩽4 s spent at any sequential depth. 'Direct ascent' involved a monotonic depth decrease with ⩽4 s at any depth. The intervening time was termed the 'hunting phase', in which depth might vary up or down, and over 4 s might be spent at one or more depths. The hunting phase sometimes included progressive descent or ascent, but at lower speeds than during direct descent or ascent. We compared model predictions of swimming speeds only with speeds during direct descent and ascent during 11 dives to depths of 56–100 m, with hunting phases of 104–124 s and a range of depths during the hunting phase of 0–5 m.

Diving birds often descend and ascend at angles less than 90 °, so that changes in depth over time cannot be used to calculate swimming speeds (Wilson et al., 1996). However, the dives of Brünnich's guillemots we studied at Coats Island appeared to be essentially vertical, with almost constant speeds during direct descent and ascent (see also Croll et al., 1992). The 11 dives we examined in detail were dives 112–122 of 123 dives made during the foraging period. Although most earlier dives were to depths of less than 40 m, apparently to feed on crustaceans in the water column (*Parathemisto*, *Mysis*, *Ischyroceros*), near the end of the foraging period guillemots typically made a short series of dives to more than 55 m, probably to capture demersal fish such as arctic cod (*Boreogadus saida*), sandlance (*Ammodytes* spp.) and sculpin (*Triglops* spp.), which were taken to chicks (Gaston and Noble, 1985; Croll, 1990). According to this pattern, dives examined in the present study were of the demersal type, with no adjustment of speeds or dive angles to maximize encounter rates in the water column (see also Thompson et al., 1993; Wilson et al., 1996). Thus, the speeds we calculated from time/depth recordings appear to represent actual swimming speeds. Patterns of swimming speeds during direct descent and ascent were very similar among the 11 dives examined, so we selected a representative dive to compare our model predictions with observed swimming speeds.

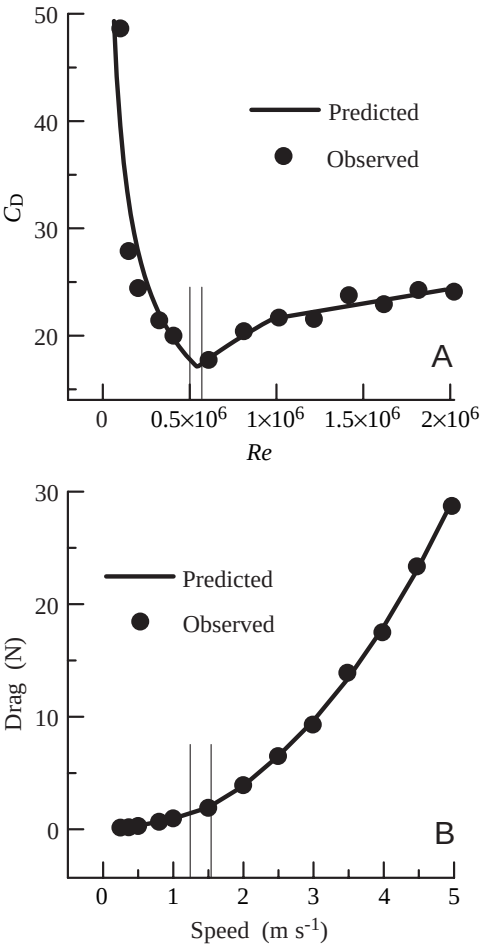

Fig. 2. (A) Drag coefficient (C_D) *versus* Reynolds number (*Re*) of a frozen common guillemot with the wings removed, the feet attached, a body length of 0.478 m and a wetted surface area of 0.0964 m^2. The curve was fitted piecewise by the following equations: for speeds <1.5 m s^{-1}, $C_D=11924.5Re^{-0.4959}$ (r^2=0.85, P=0.008); for speeds ⩾1.5 m s^{-1} and <2.5 m s^{-1}, $C_D=0.08940Re^{0.3977}$ (r^2=0.98, P=0.098); and for speeds ⩾2.5 m s^{-1}, $C_D=18.8743+2.746\times10^{-6}Re$ (r^2=0.74, P=0.027). (B) Observed values of drag on which the equations in A were based and drag predicted from those equations. An independent estimate of drag (D) at different speeds (U) is provided by the curve $D=0.371–0.872U+1.327U^2$ (r^2>0.99, P<0.001). The range of speeds and corresponding *Re* at which free-ranging guillemots swam throughout direct descent and during ascent at low positive buoyancies (≈1.52 m s^{-1}, $Re\approx0.63\times10^6$), and during ascent at negative buoyancies (≈1.25 m s^{-1}, $Re\approx0.52\times10^6$), are delineated by vertical lines (see also Figs 4, 5).

Results

Drag and buoyancy

The curve of drag coefficient (C_D) *versus Re* for the frozen common guillemot (Fig. 2A) resembled that of a bluff body (a smooth sphere or cylinder normal to the flow), with transition to fully turbulent flow at approximately $Re=0.5\times10^6$ (seen as a sharp dip; cf. Fig. 5.8 in Vogel, 1994). Because the frozen guillemot acted like a bluff body rather than a streamlined shape, the drag coefficient decreased dramatically as the separation point moved rearwards and the wide wake of turbulent eddies changed abruptly to a narrower, fully turbulent wake (Vogel, 1994). This transition is not obvious in the curve for drag itself (Fig. 2B), because the speed (U) is relatively low at the point of minimum C_D (drag=$0.5C_D\rho A_{sw}U^2$, so the effects on drag of changes in speed for U<1 m s^{-1} are small). However, it is significant that drag increases rapidly at speeds above that for minimum C_D.

With compression of air spaces by hydrostatic pressure, the calculated change in buoyancy was most rapid in the top 20 m, below which the rate of change declined dramatically (Fig. 3). On the basis of the values of body composition and air volumes we used (see Materials and methods), a guillemot weighing 1.087 kg was negatively buoyant below a depth of 62 m.

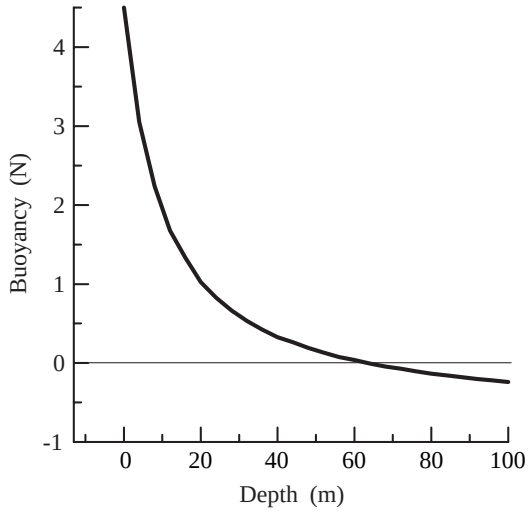

Fig. 3. Modeled change in buoyancy with depth for guillemots weighing 1.087 kg. Guillemots were negatively buoyant below a depth of 62 m.

Observed versus *predicted swimming speeds*

In films from Lancaster Sound, descending guillemots within 4 m of the water surface had a mean stroke duration of 0.357 s (a stroke rate of 2.80 Hz). Assuming a mean descent speed of 0.94 m s^{-1} (Croll et al., 1992) and buoyancy as calculated above, the modeled work in the first 2 m of descent averaged 8.15 J stroke^{-1}. If this stroke duration and work per stroke remained constant throughout descent, our model assumed that the distance per stroke and resulting speed would increase as buoyant resistance decreased. Accordingly, the modeled pattern of increasing speed during descent (solid line in Fig. 4A) resembled patterns of decreasing buoyancy (Fig. 3). Although buoyancy became increasingly negative below 62 m, the rate of change in descent speed decreased rather than increased. This pattern occurred because increased drag at higher speeds balanced the downward forces of negative buoyancy and swimming thrust, resulting in a terminal speed of 1.5–1.6 m s^{-1} at depths over 40 m.

In contrast, the instrumented guillemot reached a speed of approximately 1.52 m s^{-1} within 10 m of the water surface and maintained that speed throughout direct descent (Fig. 4) regardless of the change in buoyancy from 4.50 N at the surface to –0.15 N at 81.5 m. This pattern of quickly reaching a constant speed that was maintained throughout descent applied generally to dives of all depths throughout the foraging period (123 dives). The observed speed corresponded closely to the speed of minimum drag coefficient (C_D) for the frozen carcass (for 1.52 m s^{-1}, Re=0.63×10^6 and C_D=18.1, Fig. 2).

At the beginning of ascent, our model predicted that guillemots should actively swim upwards until the buoyancy of expanding air volumes provided an adequate speed to offset the costs of the high resting metabolic rate during passive ascent (Fig. 5). At a time step of one (constant) stroke duration, the model directed the bird to stroke or ascend passively,

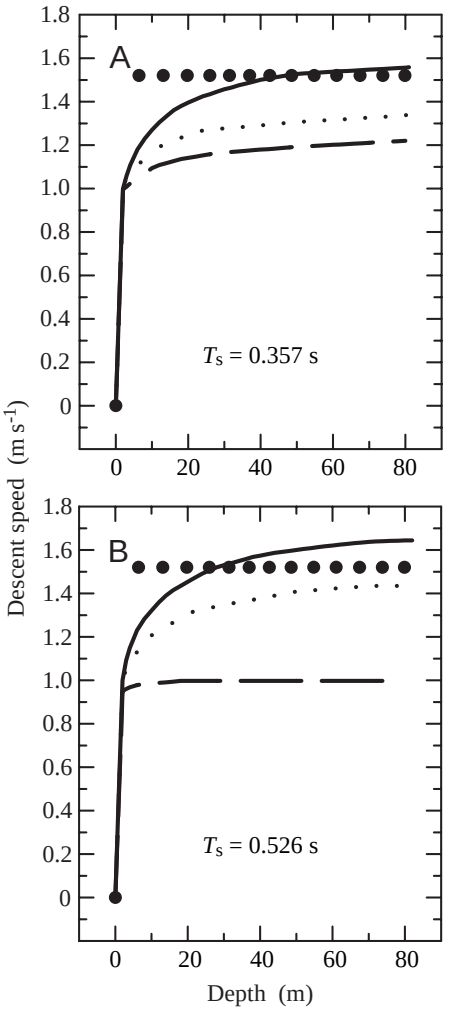

Fig. 4. Descent speed *versus* depth for guillemots predicted from the model assuming a constant stroke rate and work per stroke as buoyancy changes with depth (solid line), and speeds from a representative dive by a free-ranging Brünnich's guillemot fitted with a time/depth recorder (closed circles). Other curves show simulated speeds when the fraction of average speed occurring during the upstroke is decreased, and that during the downstroke increased, by 30 % (dots) and 60 % (dashes) (see also Fig. 1). T_s, stroke duration. (A) T_s=0.357 s; (B) T_s=0.526 s.

whichever yielded the lowest cost of transport (aerobic energy used per distance traveled, J kg^{-1} m^{-1}). During ascent, the model assumed that guillemots maintained the same stroke duration and work per stroke as observed in the first few meters of descent.

Given these assumptions, ascending guillemots should stroke steadily at 1.8 m s^{-1} below the depth of neutral buoyancy (62 m), use alternate stroking and gliding at low buoyancies from 62 to 15 m (last stroke at 19 m) and ascend passively by buoyancy alone from 15 m to the water surface (solid line in Fig. 5A). Note that buoyancy increased dramatically above approximately 20 m depth (Fig. 3). In contrast, the instrumented guillemot ascended steadily at 1.25 m s^{-1} when

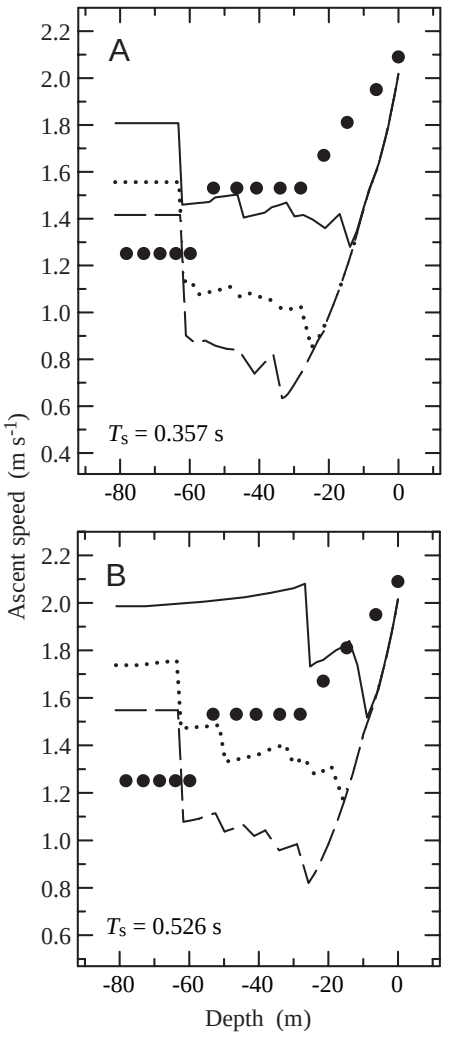

Fig. 5. Ascent speeds *versus* depth for guillemots predicted from the model assuming a constant stroke rate and work per stroke as buoyancy changes with depth (solid line), and speeds from a representative dive by a free-ranging Brünnich's guillemot fitted with a time/depth recorder (closed circles). Other curves show simulated speeds when the fraction of average speed occurring during the upstroke is decreased, and that during the downstroke increased, by 30 % (dots) and 60 % (dashes) (see also Fig. 1). Lines in the jagged phase of low buoyancies connect points for mean speeds of individual stroke–glide cycles, each averaged over a single stroke and the 1–19 time steps (stroke durations) of passive ascent that follow it before another stroke. T_s, stroke duration. (A) T_s=0.357 s; (B) T_s=0.526 s.

negatively buoyant, increased its speed to a constant 1.5 m s^{-1} at small positive buoyancies between 62 and 25 m depth, and supplemented buoyant upthrust with stroking as buoyancy increased rapidly above 25 m (i.e. the observed speed was higher than would result from buoyancy alone).

Observed ascent speeds at negative and small positive buoyancies again corresponded closely to speeds of minimum drag coefficient for the frozen carcass (for 1.25 m s^{-1}, C_D=17.5; for 1.52 m s^{-1}, C_D=18.1; Fig. 2). Predicted speed while buoyancy was negative (1.8 m s^{-1}) corresponded to a C_D of 19.4, a value 11 % greater than that observed. Although this difference in C_D is not large, the fact that the free-ranging guillemot maintained its speed within such a narrow range (vertical lines in Fig. 2) suggests substantial energetic benefits to fine adjustments of speed. These results also indicate that the guillemot maintained a net speed of optimum drag by altering either stroke rate or work per stroke as buoyancy changed with depth. After buoyancy had increased to approximately 14 % (0.63 N) of the buoyancy at the water surface (4.50 N), the guillemot supplemented buoyant upthrust with stroking to increase its ascent speed by approximately 1.17 % per meter of decreasing depth.

Variation in stroke durations and stroke acceleration curves

Comparing field and model results showed that assuming that both stroke rate and work per stroke stay constant as buoyancy changes is incorrect. As explained below, uncertainty analyses suggested important ways in which these variables might change without loss of muscle efficiency.

During descent, we altered the stroke duration of the model from 0.357 to 0.526 s, corresponding to values measured during vertical descent at shallow depths *versus* horizontal swimming, respectively. This change had no effect on the general shape of the descent speed curves with depth, but asymptotic speeds were approximately 0.1 m s^{-1} higher for the longer stroke duration (Fig. 4). A longer stroke duration means that instantaneous speed and acceleration during a stroke are lower, resulting in lower drag and inertial resistance to oppose the constant work output per stroke that we assumed. Increasing the amount of thrust provided by the downstroke *versus* the upstroke, from a moderate difference to almost all the thrust being generated on the downstroke (cf. Figs 1, 4), reduced swimming speed for the same reason: more thrust on the downstroke leads to greater instantaneous speeds during the stroke, which incur exponentially increasing drag and greater inertial work (Fig. 2).

In this regard, shortening the stroke duration and increasing the fraction of thrust on the downstroke have similar effects in decreasing the speed that minimizes the cost of transport (J kg^{-1} m^{-1}). Both these changes increase instantaneous speeds during part of the stroke (e.g. the high peak of the dashed line during the downstroke in Fig. 1). Because drag increases nonlinearly with increasing speed (Fig. 2), increased instantaneous speeds result in a net increase in total drag work. Similar mechanisms explain the differences among the curves during ascent shown in Fig. 5. Thus, the simulated curves demonstrate the potential benefits of lengthening the stroke duration and minimizing inequalities of thrust during the upstroke and downstroke, whenever buoyant resistance is low enough to allow these adjustments while maintaining ecologically effective speeds.

During ascent at low positive buoyancies (62–15 m), the model showed that alternate stroking and gliding (Fig. 5) also occurred because drag increases exponentially with increasing speed. This effect made the costs of stroking greater than the

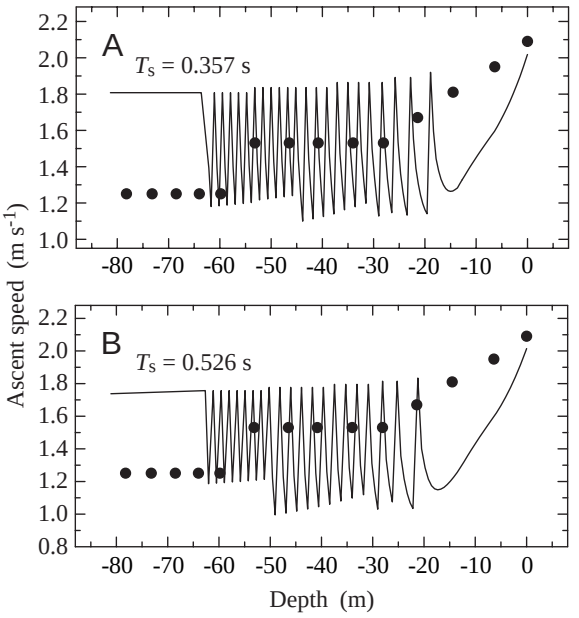

Fig. 6. Simulated ascent speeds throughout individual stroke–glide cycles, including a peak during each stroke and decreasing speed during the subsequent glide before another stroke (solid line), compared with observed speeds of a free-ranging guillemot fitted with a time/depth recorder (closed circles). The curve in A is for a stroke duration (T_s) of 0.357 s and the stroke acceleration curve indicated by the solid line in Fig. 1. The curve in B is for a T_s of 0.526 s and the stroke acceleration curve indicated by the dotted line in Fig. 1.

costs of passive ascent if more than one stroke (with accumulating higher speed and drag) occurred without separation by a passive glide. Such a strategy of alternate stroking and gliding to reduce drag costs is well known in birds flying in air (Pennycuick, 1987b, 1991) and in penguins swimming under water (Clark and Bemis, 1979). The lines in the jagged phase of low buoyancy in Fig. 5 connect points that are the mean speeds of individual stroke–glide cycles, each averaged over a single stroke and the 1–19 time steps of passive ascent that followed it before another stroke. The jagged curves indicate that the mean speeds of successive stroke–glide cycles were variable under optimized conditions.

In contrast to Fig. 5, the curves in Fig. 6 show speeds throughout individual stroke–glide cycles, with peaks representing speeds during a stroke followed by declining speeds during a glide phase before the next stroke. The curve for the shorter stroke duration with moderately greater thrust during the downstroke than the upstroke (Fig. 6A) is very similar to the curve for the longer stroke duration with an additional 30 % of total thrust during the downstroke (Fig. 6B; cf. Fig. 5). This similarity again suggests that decreasing the stroke duration has the same effect on swimming speed as increasing the fraction of thrust on the downstroke: both increase total drag and inertial work by raising instantaneous speed and acceleration during parts of the stroke.

These curves suggest that, as buoyancy changes, work per stroke can be conserved by varying the stroke duration and/or the fraction of work done during the downstroke, while maintaining the same net swimming speed. To conserve contraction speed as well as work per stroke, the bird can vary the duration of the subsequent glide phase (we do not consider the glide phase as part of the stroke, but rather as time steps following the stroke during which no strokes occur). For example, in the initial segment of the stroke–glide sequences in Fig. 6, the glide phase lasts two stroke durations (time steps) in Fig. 6A but only one stroke duration in Fig. 6B (these differences in glide duration are seen as differences in height between the highest and lowest speeds during stroke–glide cycles). However, mean speeds in the two cases differ by only approximately 0.05 m s^{-1}. Moreover, films of guillemots swimming horizontally without buoyant resistance showed a substantial glide phase following the downstroke. On the basis of these films and model simulations, there appears to be considerable flexibility for maintaining optimal speeds against varying buoyant resistance while conserving muscle contraction speeds and work during those contractions.

Discussion

Drag of frozen versus *live birds*

The drag of the frozen guillemot (Fig. 2) resembled that of a bluff body rather than a streamlined shape. Although bluff bodies exhibit dramatic reductions in drag coefficient at the transition to fully turbulent flow, their drag is still much greater than for streamlined shapes (Vogel, 1994). Pennycuick et al. (1996) suggested that the drag of frozen birds in air is higher than that of live birds because their feathers flutter unrealistically, amplify turbulence and enhance flow separation. In our experiments, feather flutter was evident at higher speeds.

However, in vertical dives by guillemots, the oscillating wings, the acceleration patterns of the fuselage and the notable pitching movements probably disrupt laminar flow over the fuselage. For cast models of penguins without feathers or oscillating movements, flow separation still occurred in the tail region and drag patterns were similar to ours for guillemots (Oehme and Bannasch, 1989; Hui, 1988). Trailing feet might substantially increase drag (Pennycuick et al., 1996), and the feet of guillemots extend well behind the short tail. Feather flutter probably inflated our measurements at the highest instantaneous speeds: for example, for the highest multiple of mean speed of 2.5 (the peak of the dashed line in Fig. 1) and a mean speed of 1.5 m s^{-1} (Figs 4, 5), the highest instantaneous speed during a stroke would be 3.75 m s^{-1}. During most of the stroke and for less extreme acceleration curves, instantaneous speeds are far lower, and this effect is less important.

Stroke acceleration curve

Because no direct data exist on fuselage speeds throughout swimming strokes in auks, we assumed a reasonable curve and varied this shape between possible extremes (Fig. 1). At present, the fraction of thrust derived from the upstroke in auks

is unknown. From a blade-element analysis of high-speed films of penguins swimming horizontally near the water surface, Hui (1988) concluded that more thrust occurred on the upstroke than the downstroke. This pattern might have resulted from the need to offset high positive buoyancy near the surface, just as birds flying in air must offset gravity by generating more thrust on the downstroke.

On the basis of bubble patterns in the wake, Rayner (1995) suggested that pigeon guillemots (*Cepphus columba*) generate most thrust with the downstroke. Certainly, the skeleton and musculature of guillemots appear to be adapted mainly for downstroke-based aerial flight (Stettenheim, 1959; Raikow et al., 1988). However, the high angles of attack during the upstroke illustrated for common guillemots by Stettenheim (1959), and in the films of Brünnich's guillemots we examined, suggest appreciable upstroke thrust under certain conditions (see also Clark and Bemis, 1979). Moreover, stroke acceleration patterns may differ between horizontal and vertical swimming in auks because descent against buoyancy is far more pulsatile. Our simulations indicate that varying the fraction of thrust arising from the upstroke *versus* the downstroke is an effective way to maintain speeds that minimize drag without losing muscle efficiency. High-speed films are desirable to document stroke acceleration patterns in auks (see also Lovvorn et al., 1991), but obtaining such data at different depths throughout deep dives will be a major challenge.

Patterns in other species

To our knowledge, our data for Brünnich's guillemots are the only records of short-term swimming speeds of diving auks. Such data are also lacking for most penguins, which tend to have shallow and more variable dive angles so that time/depth data alone cannot be converted to swimming speeds. However, direct speed measurements with an electronic logger showed that an African penguin (*Spheniscus demersus*) varied its speed with depth (Wilson and Wilson, 1995). This penguin seemed to reach a terminal speed of $2.4\,m\,s^{-1}$ between 20 and 25 m depth, but its dive angle was shallower and it approached this terminal speed more gradually than did our guillemots. Maximum dive depth for the penguin was only 30–35 m, probably well above neutral buoyancy, and it is not known whether speed would have increased with decreased buoyancy at greater depths.

Japanese cormorants (*Phalacrocorax capillatus*), king cormorants (*P. albiventer*) and South Georgian shags (*P. georgianus*) with time/depth recorders descended rapidly and directly to depths up to 45, 66 and 101 m, respectively (Kato et al., 1996; Watanuki et al., 1996; Bevan et al., 1997). Their dive profiles from readings every 1–6 s resembled those of our Brünnich's guillemots (Croll et al., 1992), suggesting that a terminal speed was reached quickly and was maintained throughout descent, rather than changing as buoyancy decreased. Further investigations are needed to determine whether their speeds corresponded to minimum drag coefficients (see. Fig. 2).

In conclusion, our biomechanical model provided testable hypotheses for locomotion by guillemots. Calculated swimming speeds based on constant stroke frequency and work per stroke as buoyancy changed did not agree with speeds recorded from a free-ranging guillemot. Rather, the guillemot maintained its speed within a narrow range that minimized the drag coefficient. In films, stroke frequency during descent against high buoyancy was greater than that during horizontal swimming, which had a substantial glide phase. These data and model simulations suggest that guillemots can modulate their swimming speeds, without altering their contraction speeds or work per contraction, by varying their stroke duration, the relative thrust on the downstroke *versus* the upstroke, and the duration of gliding. Given the potential use of heat from inefficient muscles for thermoregulation, guillemots can probably sustain speeds that optimize mechanical efficiency (drag) with little change in net physiological efficiency. Continued miniaturization of instruments to record depths, swimming speeds, electromyograms of stroke rates, and accelerometer readings throughout deep dives (see also Dial, 1992; Kooyman et al., 1992; Bevan et al., 1997; Y. Watanuki, personal communication) would help to confirm our results and refine biomechanical models for auk-sized birds.

We thank G. V. Byrd and A. L. Sowls for obtaining guillemot specimens and G. Stensgaard of the BC Research Ocean Engineering Center for access to the drag tank. M. H. Borstad, J. Mikkelsen and A. Akinturk gave us critical help with drag measurements, and S. M. Calisal and D. R. Jones generously provided laboratory space. A. J. Gaston greatly facilitated the work at Coats Island and drew our attention to the films of diving guillemots. E. McLaren provided invaluable field assistance. J.R.L. was supported by US National Science Foundation grant OPP-9813979 and a contract with the Ecological Services Division of the US Fish and Wildlife Service. D.A.C. was supported by US National Institutes of Health grant HL 17731 to G. L. Kooyman and US Office of Naval Research Grant N00014-95-10646.

References

Bevan, R. M., Boyd, I. L., Butler, P. J., Reid, K., Woakes, A. J. and Croxall, J. P. (1997). Heart rates and abdominal temperatures of free-ranging South Georgian shags, *Phalacrocorax georgianus*. *J. Exp. Biol*. **200**, 661–675.

Bevan, R. M. and Butler, P. J. (1992). The effects of temperature on the oxygen consumption, heart rate and deep body temperature during diving in the tufted duck *Aythya fuligula*. *J. Exp. Biol.* **163**, 139–151.

Bruinzeel, L. W. and Piersma, T. (1998). Cost reduction in the cold: heat generated by terrestrial locomotion partly substitutes for thermoregulation costs in knot *Calidris canutus*. *Ibis* **140**, 323–328.

Chai, P., Chang, A. C. and Dudley, R. (1998). Flight thermogenesis and energy conservation in hovering hummingbirds. *J. Exp. Biol*. **201**, 963–968.

Clark, B. D. and Bemis, W. (1979). Kinematics of swimming of penguins at the Detroit Zoo. *J. Zool., Lond*. **188**, 411–428.

Croll, D. A. (1990). Diving and energetics of the thick-billed murre, *Uria lomvia*. PhD thesis, University of California, San Diego, USA.

Croll, D. A., Gaston, A. J., Burger, A. E. and Konnoff, D. (1992). Foraging behavior and physiological adaptation for diving in thick-billed murres. *Ecology* **73**, 344–356.

Croll, D. A. and McLaren, E. (1993). Diving metabolism and thermoregulation in common and thick-billed murres. *J. Comp. Physiol.* B **163**, 160–166.

Culik, B. and Wilson, R. P. (1991). Energetics of under-water swimming in Adélie penguins (*Pygoscelis adeliae*). *J. Comp. Physiol.* B **161**, 285–291.

DeVries, A. L. and Eastman, J. T. (1978). Lipid sacs as a buoyancy adaptation in an Antarctic fish. *Nature* **271**, 352–353.

Dial, K. P. (1992). Activity patterns of the wing muscles of the pigeon (*Columba livia*) during different modes of flight. *J. Exp. Zool*. **262**, 357–373.

Furness, R. W., Thompson, D. R. and Harrison, N. (1994). Biometrics and seasonal changes in body composition of common guillemots *Uria aalge* from north-west Scotland. *Seabird* **16**, 22–29.

Gaston, A. J. and Noble, D. G. (1985). The diet of thick-billed murres (*Uria lomvia*) in west Hudson Strait and northeast Hudson Bay. *Can. J. Zool*. **63**, 1148–1160.

Goldspink, G. (1977). Mechanics and energetics of muscle in animals of different sizes, with particular reference to the muscle fibre composition of vertebrate muscle. In *Scale Effects in Animal Locomotion* (ed. T. J. Pedley), pp. 37–55. London: Academic Press.

Goldspink, G. (1981). The use of muscles during flying, swimming and running from the point of view of energy saving. *Symp. Zool. Soc. Lond.* **48**, 219–238.

Grémillet, D., Tuschy, I. and Kierspel, M. (1998). Body temperature and insulation in diving great cormorants and European shags. *Funct. Ecol*. **12**, 386–394.

Hawkins, P. A. J., Butler, P. J., Woakes, A. J. and Gabrielsen, G. W. (1997). Heat increment of feeding in Brünnich's guillemot *Uria lomvia*. *J. Exp. Biol.* **200**, 1757–1763.

Hill, A. V. (1950). The dimensions of animals and their muscular dynamics. *Science Prog.* **38**, 209–230.

Hill, A. V. (1964). The efficiency of mechanical power development during muscular shortening and its relation to load. *Proc. R. Soc. Lond. B* **159**, 319–324.

Hind, A. T. and Gurney, W. S. C. (1997). The metabolic cost of swimming in marine homeotherms. *J. Exp. Biol*. **200**, 531–542.

Hui, C. A. (1988). Penguin swimming. I. Hydrodynamics. *Physiol. Zool.* **61**, 333–343.

Kato, A., Naito, Y., Watanuki, Y. and Shaughnessy, P. D. (1996). Diving pattern and stomach temperatures of foraging king cormorants at subantarctic Macquarie Island. *Condor* **98**, 844–848.

Keijer, E. and Butler, P. J. (1982). Volumes of the respiratory and circulatory systems in tufted and mallard ducks. *J. Exp. Biol.* **101**, 213–220.

Kooyman, G. L., Gentry, R. L., Bergman, W. P. and Hammel, H. T. (1976). Heat loss in penguins during immersion and compression. *Comp. Biochem. Physiol.* A **54**, 75–80.

Kooyman, G. L., Ponganis, P. J., Castellini, M. A., Ponganis, E. P., Ponganis, K. V., Thorson, P. H., Eckert, S. A. and LeMaho, Y. (1992). Heart rates and swim speeds of emperor penguins diving under sea ice. *J. Exp. Biol*. **165**, 161–180.

Lasiewski, R. C. and Calder, W. A. (1971). A preliminary allometric analysis of respiratory variables in resting birds. *Respir. Physiol*. **11**, 152–166.

Leafloor, J. O., Thompson, J. E. and Ankney, C. D. (1996). Body mass and carcass composition of fall migrant oldsquaws. *Wilson Bull*. **108**, 567–572.

Lovvorn, J. R. (1991). Mechanics of underwater swimming in foot-propelled diving birds. *Proc. Int. Ornithol. Congr.* **20**, 1868–1874.

Lovvorn, J. R. (1994). Biomechanics and foraging profitability: an approach to assessing trophic needs and impacts of diving ducks. *Hydrobiologia* **279/280**, 223–233.

Lovvorn, J. R. and Jones, D. R. (1991a). Effects of body size, body fat, and change in pressure with depth on buoyancy and costs of diving in ducks (*Aythya* spp.). *Can. J. Zool.* **69**, 2879–2887.

Lovvorn, J. R. and Jones, D. R. (1991b). Body mass, volume, and buoyancy of some aquatic birds and their relation to locomotor strategies. *Can. J. Zool.* **69**, 2888–2892.

Lovvorn, J. R. and Jones, D. R. (1994). Biomechanical conflicts between adaptations for diving and aerial flight in estuarine birds. *Estuaries* **17**, 62–75.

Lovvorn, J. R., Jones, D. R. and Blake, R. W. (1991). Mechanics of underwater locomotion in diving ducks: drag, buoyancy and acceleration in a size gradient of species. *J. Exp. Biol.* **159**, 89–108.

National Geographic Society (1995). *Arctic Kingdom: Life at the Edge*. National Geographic Society, Washington, DC, USA (television film).

Oehme, H. and Bannasch, R. (1989). Energetics of locomotion in penguins. In *Energy Transformations in Cells and Organisms* (ed. W. Wieser and E. Gnaiger), pp. 230–240. Proceedings of the 10th Conference of the European Society for Comparative Physiology and Biochemistry. New York, Stuttgart: Georg Thiem Verlag.

Pennycuick, C. J. (1987a). Flight of auks (Alcidae) and other northern seabirds compared with southern Procellariiformes: ornithodolite observations. *J. Exp. Biol*. **128**, 335–347.

Pennycuick, C. J. (1987b). Flight of seabirds. In *Seabirds: Feeding Ecology and Role in Marine Ecosystems* (ed. J. P. Croxall), pp. 43–62. Cambridge: Cambridge University Press.

Pennycuick, C. J. (1990). Predicting wingbeat frequency and wavelength of birds. *J. Exp. Biol*. **150**, 171–185.

Pennycuick, C. J. (1991). Adapting skeletal muscle to be efficient. In *Efficiency and Economy in Animal Physiology* (ed. R. W. Blake), pp. 33–42. Cambridge: Cambridge University Press.

Pennycuick, C. J. (1992). *Newton Rules Biology*. Oxford: Oxford University Press.

Pennycuick, C. J. (1996). Wingbeat frequency of birds in steady cruising flight: new data and improved predictions. *J. Exp. Biol*. **199**, 1613–1618.

Pennycuick, C. J. (1997). Actual and 'optimum' flight speeds: field data reassessed. *J. Exp. Biol.* **200**, 2355–2361.

Pennycuick, C. J., Klaassen, M., Kvist, A. and Lindstrom, A. (1996). Wingbeat frequency and the body drag anomaly: wind-tunnel observations on a thrush nightingale (*Luscinia luscinia*) and a teal (*Anas crecca*). *J. Exp. Biol*. **199**, 2757–2765.

Raikow, R. J., Bicanovsky, L. and Bledsoe, A. H. (1988). Forelimb joint mobility and the evolution of wing-propelled diving in birds. *Auk* **105**, 446–451.

Raveling, D. G. (1979). The annual cycle of body composition of Canada geese with special reference to control of reproduction. *Auk* **96**, 234–252.

Rayner, J. M. V. (1995). Dynamics of the vortex wakes of flying and swimming vertebrates. In *Biological Fluid Dynamics* (ed. C. P. Ellington and T. J. Pedley), *Symp. Soc. Exp. Biol.* **49**, 131–155.

Rome, L. C., Funke, R. P., Alexander, R. McN., Lutz, G., Aldridge, H., Scott, F. and Freadman, M. (1988). Why animals have different muscle fibre types. *Nature* **335**, 824–827.

Stephenson, R. (1994). Diving energetics in lesser scaup (*Aythya affinis*, Eyton). *J. Exp. Biol*. **190**, 155–178.

Stephenson, R. (1995). Respiratory and plumage gas volumes in unrestrained diving ducks (*Aythya affinis*). *Respir. Physiol.* **100**, 129–137.

Stephenson, R., Lovvorn, J. R., Heieis, M. R. A., Jones, D. R. and Blake, R. W. (1989a). A hydromechanical model of the power requirements of diving and surface swimming in lesser scaup (*Aythya affinis*). *J. Exp. Biol.* **147**, 507–519.

Stephenson, R., Turner, D. L. and Butler, P. J. (1989b). The relationship between diving activity and oxygen storage capacity in the tufted duck (*Aythya fuligula*). *J. Exp. Biol.* **141**, 265–275.

Stettenheim, P. (1959). Adaptations for underwater swimming in the common murre (*Uria aalge*). PhD thesis, University of Michigan, Ann Arbor, USA.

Swennen, C. and Duiven, P. (1991). Diving speed and food-size selection in common guillemots, *Uria aalge*. *Neth. J. Sea Res.* **27**, 191–196.

Thompson, D., Hiby, A. R. and Fedak, M. A. (1993). How fast should I swim? Behavioural implications of diving physiology. *Symp. Zool. Soc. Lond*. **66**, 349–368.

Torrella, J. R., Fouces, V., Palomeque, J. and Viscor, G. (1996). Capillarity and fibre types in locomotory muscles of wild mallard ducks (*Anas platyrhynchos*). *J. Comp. Physiol.* B **166**, 164–177.

Turner, D. L. and Butler, P. J. (1988). The aerobic capacity of locomotory muscles in the tufted duck, *Aythya fuligula*. *J. Exp. Biol*. **135**, 445–460.

Vogel, S. (1994). *Life in Moving Fluids*. 2nd edn. Princeton: Princeton University Press.

Watanuki, Y., Kato, A. and Naito, Y. (1996). Diving performance of male and female Japanese cormorants. *Can. J. Zool*. **74**, 1098–1109.

Wilson, R. P., Culik, B. M., Peters, G. and Bannasch, R. (1996). Diving behaviour of gentoo penguins, *Pygoscelis papua*; factors keeping dive profiles in shape. *Mar. Biol*. **126**, 153–162.

Wilson, R. P., Hustler, K., Ryan, P. G., Burger, A. E. and Noldeke, E. C. (1992). Diving birds in cold water: do Archimedes and Boyle determine energetic costs? *Am. Nat.* **140**, 179–200.

Wilson, R. P. and Wilson, M.-P. T. (1995). The foraging behaviour of the African penguin *Spheniscus demersus*. In *The Penguins* (ed. P. Dann, I. Norman and P. Reilly), pp. 244–265. Chipping Norton, NSW: Surrey Beatty & Sons.